Development of Steel Pipe Pile Combined with Ground Improvement in Narrow Spaces

K. Watanabe[1], T. Yamamoto[2] and T. Sudo[3]
[1]*Geotechnical Engineering Department, Technical Research Institute, Obayashi Corporation, Tokyo, Japan*
[2]*Design Department, Obayashi Corporation, Tokyo, Japan*
[3] *Specialty Construction Department, Obayashi Corporation, Tokyo, Japan*
E-mail: watanabe.koji.ro@obayashi.co.jp

ABSTRACT: In recent years, works to improve existing structures and strengthen their seismic resistance have increased. Pile construction in narrow spaces is constrained by the site and process. Therefore, a construction method combining steel pipe piles with ground improvement using a mechanical agitator (e-column construction method®) was developed. This paper briefly summarizes the construction method, presents the static load tests and rapid load tests, and discusses the results of load tests. The results of the loading tests suggest that the bearing capacity can be evaluated by using the undrained shear strength and SPT N-value. Also, a simplified rapid loading test can be applied to validating the bearing capacity at a construction site. For the joint of the steel pipe piles, the maximum tensile resistance obtained from the experiment was larger than that obtained from the calculation formula.

KEYWORDS: Steel pipe pile, Ground improvement, Bearing capacity, Full scale load test

1. INTRODUCTION

There are several pile construction methods with relatively small construction machinery that are suitable for construction in narrow urban spaces and areas with low overhead clearance. The Top-drill Boring Hole (TBH) method, which has a machine height of 4.5 m, is often used. However, there are many cases where even these construction machines are interfered with by architectural limitations and existing structures. In particular, piles near railway tracks or on rail platforms are currently constructed after temporary construction is carried out to ensure construction space. The Boring Hole (BH) pile method can handle narrow spaces and low overhead clearances better than the TBH method. However, because the BH pile method is a direct circulation method, mud cakes easily form on the hole walls, and slime tends to accumulate at the pile tip. This lowers the bearing capacity of the piles, so subsidence is more likely to occur. Such challenges related to the construction method, bearing capacity and settlement need to be resolved for pile construction in narrow urban spaces.

Pile construction in narrow urban spaces and for existing structures to strengthen the seismic resistance is subjected to constraints on the construction site and process. Especially, this pile is subjected to the lack of bearing capacity due to the increase of superstructure weight by strengthening the superstructure. Furthermore, noise and industrial waste need to be considered with regard to their effects on the surrounding environment. Therefore, a method for steel pipe pile construction combined with ground improvement was developed that uses a compact mechanical agitator for pile foundations of lightweight structures (Watanabe et al, 2011 and Yamamoto et al, 2011). As shown in Figure 1 (a) ~ (c), the construction machine is a mechanical agitator (e-column construction method®) with an attached vibrating mechanism and improved drilling capacity. This e-column construction machine can be used to realize pile construction in narrow spaces where construction is usually difficult. This method is characterized by having no need to drill up to a fixed depth as in the pre-boring pile construction method. Instead, soil is agitated along with the cement milk at the original position. This greatly reduces the spoil generated by pile construction. In this method, the drilling rod of the e-column machine is sent down to the bearing stratum; after agitating and mixing, the pile is composed of segmental steel pipes that are connected with bolts on flanges.

In this study, static loading tests and rapid loading tests on steel pipe piles that were constructed with the e-column construction method were carried out to evaluate the bearing capacity. Furthermore, it was evaluated the performance of the steel pipe pile joints in terms of the tensile strength.

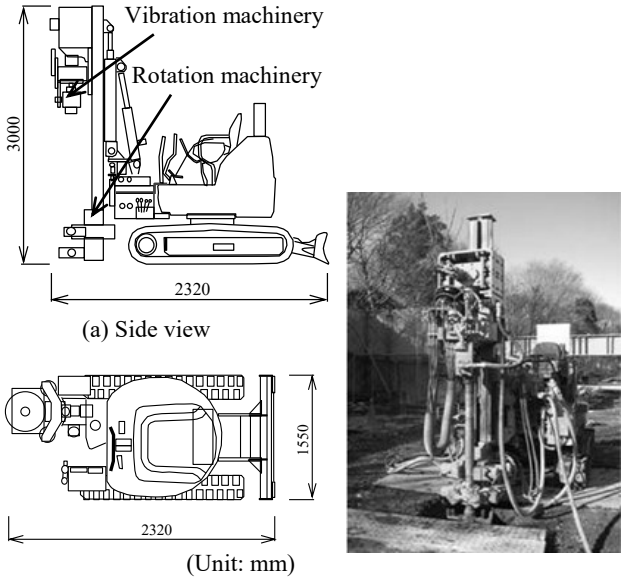

Figure 1 Machine for e-column construction method

2. OVERVIEW OF STEEL PIPE PILES COMBINED WITH GROUND IMPROVEMENT

This construction method uses two types of piles: end-bearing pile and frictional pile. These differ according to the shape of the pile tip and target strength of the soil cement, which is the ground improvement structure. For the bearing pile, the target strength of the soil cement is 0.1 N/mm^2. As shown in Figure 2(a), the flange on the pile tip is positioned on the bearing stratum, while the steel pipe is embedded 50 mm inside the bearing stratum. For the frictional pile, the target strength is 1.0 N/mm^2. As shown in Figure 2(b), the pile tip is installed inside the ground improvement structure built from soil cement. For the steel pipe pile joints, flanges are provided on both ends of the steel pipe, and the flanges are joined by bolts (see Figure 5). Because the piles constructed with this method were assumed to be for construction in narrow spaces, the steel pipes are

joined by short pieces into lengths of 1.0–1.5 m. In order to make such short joints, there should be a joint flange with a pitch of 1.0–1.5 m. This flange ensures that the steel pipe pile adheres to the soil cement. The piles were used to be fabricated from JIS standard STK steel pipe to ensure a low cost and certain level of quality.

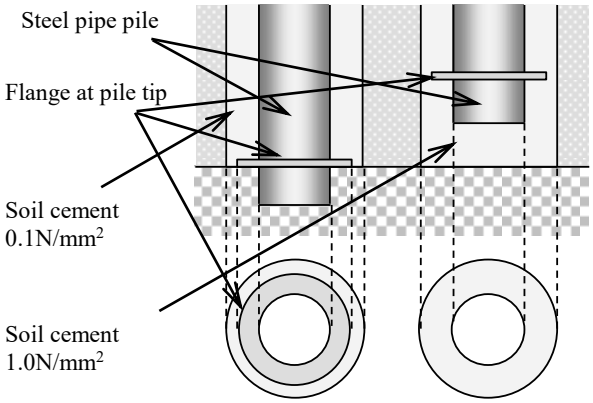

Figure 2 Pile tip shapes

The typical construction process with this method is described as follows.

1) Excavate to the bearing stratum, carry out agitation and mixing, and lay the soil cement as the ground improvement structure. During this time, carry out drilling so that the rod will reach a predetermined depth.
2) Build steel pipe pile joints in the ground improvement structure,which is in loose and poorly lithified soil.
3) For the end-bearing piles, after the steel pipe piles are built to a pile length, use the vibration mechanism of the e-column construction machine to penetrate the steel pipe pile through the bearing stratum.
4) After the pile construction is completed, carry out simplified rapid load tests to verify the bearing capacity if necessary. However, the piles should be loaded to the equivalent long-term load if the real pile behaviour has to be determined.

The above construction can be carried out using only the e-column construction machine shown in Figure 1 (a) ~ (c). The planar dimensions of the construction machine are extremely compact: a 1.55m width and 2.32m length. In addition, the construction machine is 3.0m tall, including the leader. Thus, construction is possible even with low overhead clearances. The machine has a vibration mechanism to improve the agitation and mixing capability. The results of construction test showed that even sand with an N value of about 40–50 can be agitated and mixed (Kitade et al., 2012).

3. FULL-SCALE LOAD TEST

Figure 3 shows the soil profile and test pile. The test ground was composed of loam and tuffaceous clay up to about GL −7.0 m and sand gravel and fine sand below that. Table 1 presents the physical test results and unconfined compression test results for the clayey soil layer. The unconfined compressive strength of GL −1.5 to −6.0 m was 30–89 kN/m^2.

Four piles were constructed for the static load test: three with end-bearing pile specifications and one with frictional pile specifications. The bearing stratum was adopted to be N = 10, 20, 30 from the results of ground investigation; the test end-bearing piles were embedded in the bearing stratum. The test frictional pile was embedded in the ground with about N = 10 at the pile tip. Figure 4 shows the arrangement of the test and reaction piles. Similar to the static load test, four piles were also constructed for the rapid load test: three with end-bearing pile specifications and one with

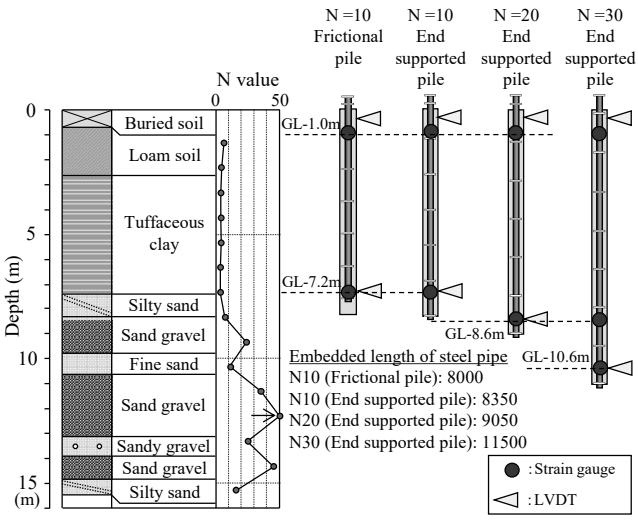

Figure 3 Soil profile and test conditions

Table 1 Results of physical tests and unconfined compression tests

Depth (GL -m)	Soil	Wet density (kN/m^3)	Natural water content w_n (%)	Unconfined compression strength q_u (kN/m^2)
1.5~2.5	Loam soil	13.034	107.4	36
3.0~4.0	Tuffaceous clay	16.562	52.9	89
5.0~6.0	Tuffaceous clay	16.366	55.4	30

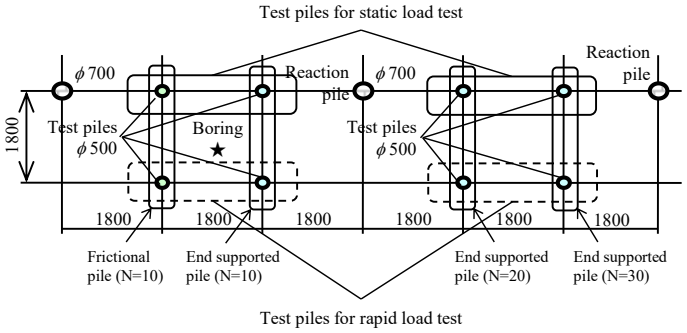

Figure 4 Arrangement of test and reaction piles

frictional pile specifications. The test piles were steel pipes with a pre-drilling soil-cement column diameter of 500mm, flange diameter of 305mm, shaft diameter of 190.7mm, and pipe thickness of t=5.3mm. The target strength of the pre-drilled soil cement as the improved ground structure was 0.1N/mm^2 with the end-bearing pile specifications and 1.0N/mm^2 with the frictional pile specifications. Based on the results of the formulation tests carried out beforehand using soil collected from the original ground, the unit quantity of cement corresponding to the target strength was taken to be 120kg/m^3 for the end-bearing piles and 250kg/m^3 for the frictional pile. In the core strength test carried out after the load test, the average strengths with the end-bearing and frictional piles were 0.15 and 2.2N/mm^2, respectively. This confirms that the target strength was satisfied. Figure 5 shows the details of the joint of the test pile.

At the joint, the two flanges were connected with a torque shear bolt (S10T, M20).

The static load test was carried out based on the standards of the Japanese Geotechnical Society ("Methods for vertical load test of piles") (2001). A stepwise multi-cycle loading system was employed with a new load holding period of 30min, hysteretic load holding duration of 2min, and zero load holding duration of 2min.

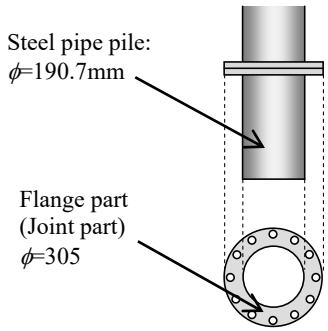

Figure 5 Details of joint part for steel pipe

The measured parameters were the pile head load, pile head and pile tip displacements, and strain of the steel pipe. The pile tip displacement was measured with the pipe-in-pipe method (i.e. double steel tube method). Similar to the static load test, the rapid loading test was also carried out based on the standards of the Japanese Geotechnical Society ("Methods for vertical load test of piles"). The rapid load test used the falling mass load method with a mass of 9.8kN. The relative loading duration Tr of the rapid loading test is defined as follows:

$$Tr = tL/(2L/c) \geq 5 \quad (1)$$

where tL is the loading duration, L is the pile length, and c is the propagation velocity of a longitudinal wave.

For the relative loading duration when the pile length is 11.5m (N=30 end-bearing pile), Tr = 9.35. Because this load test satisfied the relation Tr ≥ 5 prescribed in the standards of the Japanese Geotechnical Society, the influence of wave propagation phenomena could be neglected. The measured parameters were the pile head displacement, acceleration that occurs in the pile head, and strain of the steel pipe.

In addition to the usual falling mass loading method, we also verified the applicability of the simplified rapid load tests used for quality control after construction. Photo 1 shows the sensor used in the simplified rapid load test, and Figure 6 shows the measurement system of the rapid load test. In a typical rapid load test, the load that occurs at the pile head, the acceleration, and the displacement are measured. In contrast, in the simplified rapid load test, a single sensor with an integrated load cell and accelerometer is installed at the pile head for measurements.

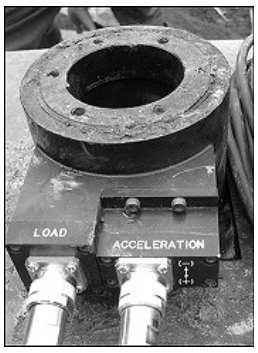

Photo 1 Sensor for simplified rapid load test

Two types of measurement system were sat to the test piles to compare the results between typical rapid load test and simplified rapid load test because the simplified rapid load test is applied to verify the bearing capacity after the construction of pile on site. With this system, when the measured data are obtained, automatic calculations can be performed simultaneously to obtain the relationship between the static load and displacement. The displacement is calculated from the second-order integral of the acceleration. The sensor used in this simplified rapid load test was used to have a maximum loading capacity of 250kN, which corresponded to the long-term bearing capacity of the assumed pile. The quality of the pile was also considered for the quality control at the site; this was limited to verifying the long-term load at the pile head and the initial stiffness. The unloading point method was adopted to calculate the static loads in both the rapid load test and simplified rapid load test. In the unloading point method, the static load is calculated by eliminating the dynamic resistance component from the obtained load.

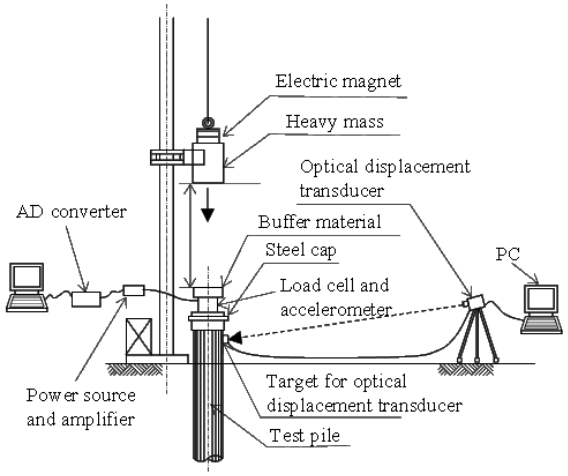

Figure 6 Measurement system for rapid loading test

4. RESULTS OF FULL SCALE LOAD TESTS

Figure 7 shows the relationships between the load and displacement at the pile head. The maximum loads were 380, 720, 1280, and 620kN. For all of the piles, the curve was steep from the initial of loading; all of the piles possessed a large initial stiffness. The gradient of the curve then changed with the loading and reached the maximum load. For the end-bearing piles, a larger N value for the -bearing stratum meant a higher stiffness. For the frictional pile, the stiffness corresponded to the stiffness of the bearing pile for a bearing stratum of N=20.

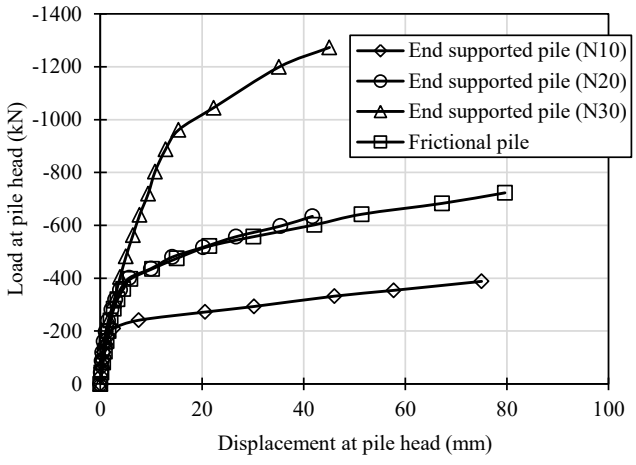

Figure 7 Relationships between Load and displacement at pile head

Figures 8 (a)~(d) show the axial force distributions of each pile. The axial force was calculated by considering only the steel pipe; the strain of the steel pipe obtained from the test was multiplied with the Young's modulus and cross-sectional area of the steel pipe. For the end-bearing piles, the axial force reaching the pile tip increased with the load and exhibited the behaviour of end-bearing piles. For the frictional pile, the axial force difference increased with increasing the applied load. Here, the reason why the maximum load

(1040kN) occurred at depth of 1m below rather than the pile head is that the buckling behaviour occurred at 1m below of the pile.

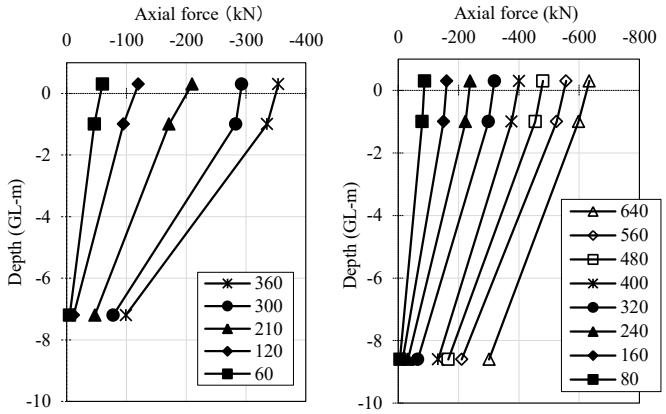

(a) End supported pile (N=10) (b) End supported pile (N=20)

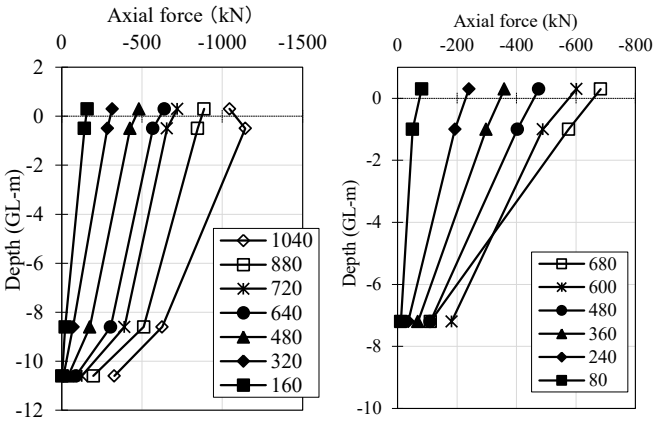

(c) End supported pile (N=30) (d) Frictional pile

Figure 8 Axial force distributions

Figure 9 shows the relationships between the displacement and shaft friction, which was obtained by dividing this axial force difference by the circumferential area. The improved diameter of the soil cement (i.e. outer diameter of soil cement column) was used when calculating the circumferential area of the friction pile.

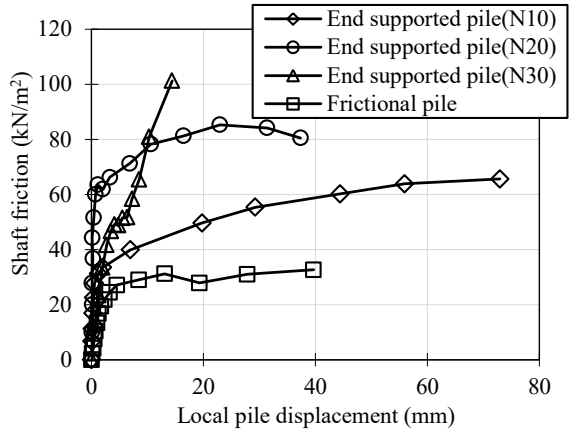

Figure 9 Relationships between shaft friction and local pile displacement

This is because the flange used in the steel pipe joint enhances the adhesion of the steel pipe to the soil cement. Because the soil cement is stronger than the end-bearing pile, it can be inferred that this system shows the behaviour of a single unified body. For the end-bearing piles, the circumferential area was calculated using the axial diameter of the steel pipe. Figure 9 shows that a maximum shaft friction of 31 ~ 100kN/m^2 was reached. In comparison, the average value for the unconfined compressive strength of the corresponding section of the ground was 51kN/m^2. Thus, it can be concluded that the shaft friction was more than the undrained shear strength of the ground (=26kN/m^2).

Figure 10 shows the relationships between the bearing capacity and displacement at pile tip. The bearing capacity was calculated by dividing the axial force reaching the pile tip by the area of the steel pipe flange near the pile tip inside the soil cement (i.e., the ground improvement structure) or bearing stratum. If the reference displacement at pile tip is 10% of the steel pipe flange diameter (i.e., maximum displacement when the displacement does not reach the reference displacement), the end-bearing piles showed large bearing capacities of 1600, 5800, and 9800kN/m^2, and the frictional pile showed a large bearing capacity of 3500kN/m^2. Here, the flange near the pile tip showed resistance to the soil cement; this may be why the bearing capacity of the frictional pile was larger than that of the end-bearing piles embedded in the same ground. This means that the steel pile and soil-cement column act as one unified body and therefore the bigger base of the unified body gives higher end bearing capacity.

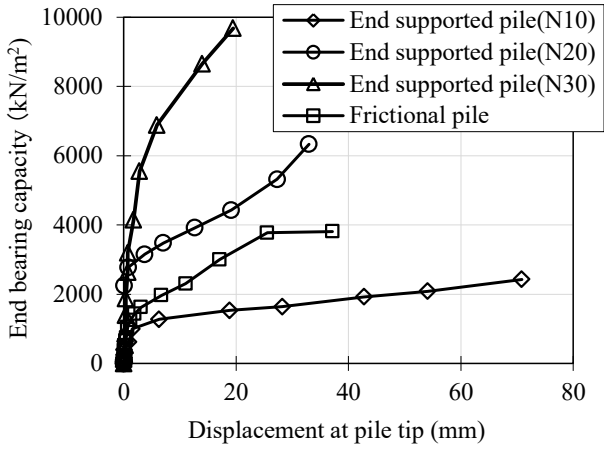

Figure 10 Relationships between end bearing capacity and Displacement at pile tip

Figure 11 shows the relationship between the ultimate bearing capacity and the N value of the bearing stratum of the ground. It is confirmed that the bearing capacity factor had a value of more than 150 for each pile. The bearing capacity characteristics developed by this construction method are given in Eqs. (2) and (3). This method develops an ultimate shaft friction and ultimate bearing capacity that are more than those of the cast-in-place concrete pile given in "Architectural Institute of Japan: Recommendation for Design of Building foundations" (2001).

Ultimate shaft friction:

$$\text{Clayey soil: } \tau = c_u \text{ (kN/m}^2\text{)} \quad (2)$$

where, τ is the shaft friction that occurs in clayey soil (kN/m^2) and c_u is the undrained shear strength of the corresponding section (kN/m^2).

Ultimate bearing capacity:

$$\text{Sandy soil: } p_b = 150N \text{ (kN/m}^2\text{)} \quad (3)$$

where p_b is the bearing capacity of the pile tip (kN/m^2) and N is the N value of the bearing stratum of the pile tip.

From the above Eqs. (4) and (5) give the formula to calculate the ultimate bearing capacity.

End-bearing pile:

$$Q_e = \tau \cdot e \cdot Le + p_b \cdot A_f \text{ (kN)} \quad (4)$$

where Q_e is the ultimate bearing capacity of the bearing pile (kN), e is the circumference of the steel pipe shaft (m), L_e is the length of the steel pipe pile (m), and A_f is the area of the flange (m^2).

Frictional pile:

$$Q_e = \tau \cdot f \cdot L_f + p_b \cdot A_f \text{ (kN)} \quad (5)$$

where Q_f is the ultimate bearing capacity of the friction pile (kN), f is the circumference of the soil cement ground improvement structure (m), L_f is the length of the soil cement ground improvement structure (m), and A_f is the area of the flange (m^2).

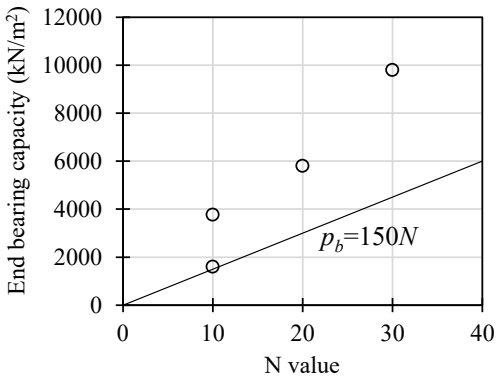

Figure 11 Relationship between end bearing capacity and N value

Figure 12 shows the adopted loading cycle. The load applied on the pile was adjusted by varying the drop height to 0.25–2.25 m.

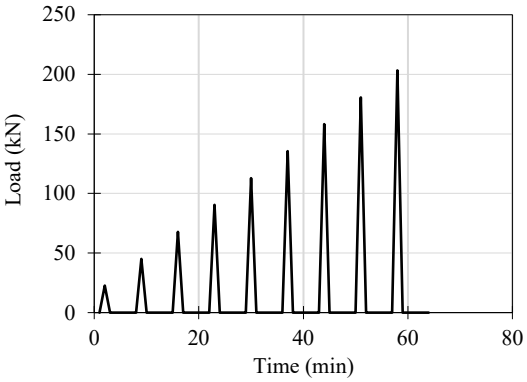

Figure 12 Load cycles of rapid load test

Figure 13 shows the relationships between the load and displacement at the pile head for each pile type. These figures show the results of the rapid load test, simplified rapid load test, and the static load test for comparison. Here, the rapid load test and the simplified rapid load test are to estimate lower than the peal load (i.e. ultimate bearing capacity). Thus, the comparison of the load and displacement relations were carried out until the load which was obtained at the pile head reached the peak value. The maximum loading values in the simplified rapid load test were confined to 150–250kN. This was because of the capacity limitations of the sensor integrated with the accelerometer used in the simplified rapid load test. For the load–displacement relationships at each pile head,

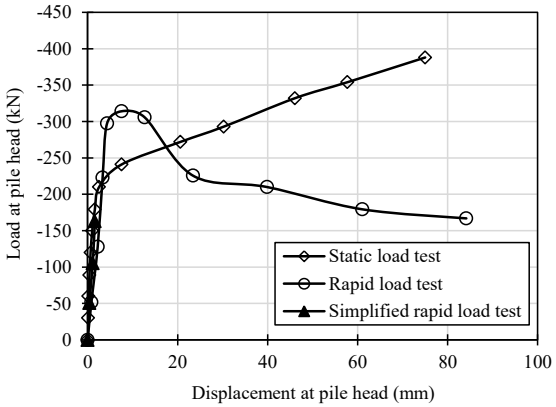

(a) End supported pile (N=10)

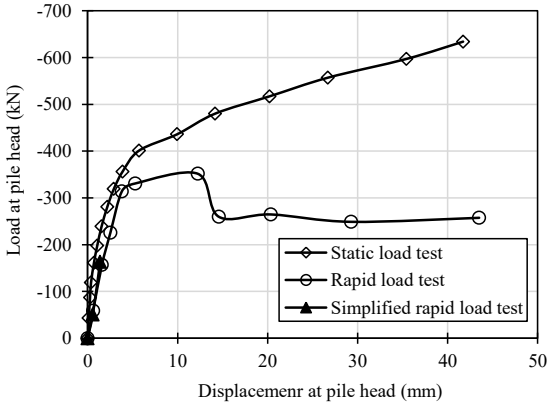

(b) End supported pile (N=20)

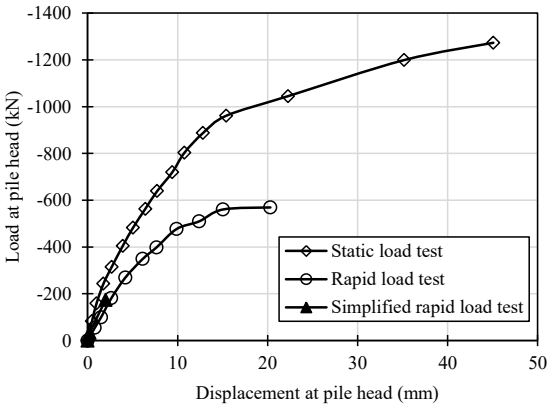

(c) End supported pile (N=30)

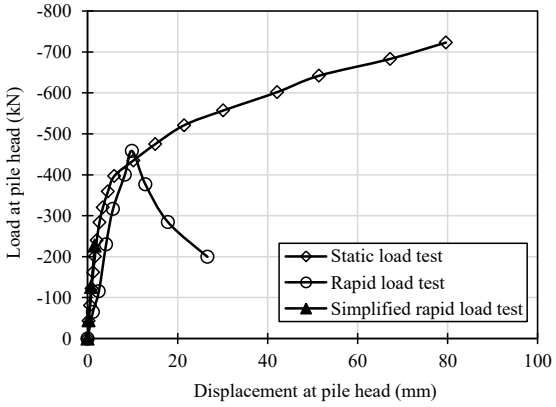

(d) Frictional pile

Figure 13 Relationships between load and displacement at pile head

although there was a slight difference in the initial stiffness of the end-bearing pile (particularly for N30 case), the results of the static load, rapid load and simplified rapid load tests were almost consistent within the loading capacity range of the sensor (250kN) and showed sufficient accuracy. Particularly for the simplified rapid load test, because the displacement was calculated from the second-order integral of the acceleration, it was concerned that there would be some difference when compared to the actually measured displacement. However, the results of the load tests showed the impact to be small. Consequently, the test results were obtained that were almost consistent with those of conventional rapid loading tests within the maximum loading range of 250kN. Thus, the simplified rapid loading test is sufficient for quality control at a construction site.

5. STUDY ON STEEL PIPE PILE JOINT

5.1 Overview of tensile loading test on steel pipe pile joint

The joint of the steel pipe pile combined with ground improvement from a design perspective to increase the maximum strength of the steel pipe is studied in this chapter. It is assumed that the developed pile only showed resistance in the vertical direction and did not bear any horizontal force. A tensile test in order to verify the strength of the joint was carried out.

Prior to the tensile loading test of the joint, we carried out a material test (tensile test) to study the mechanical properties of the steel pipe. The material test pieces conformed to the Japanese Industrial Standards (JIS-Z-2201). Table 2 lists the material test results.

Table 2 Results of material tests

	Yield resistance (N/mm^2)	Tensile strength (N/mm^2)	Breaking elongation (%)
1	394.9	483.0	38.8
2	407.8	495.2	41.3
3	410.8	486.3	39.6
Ave.	404.5	488.2	39.9

A test specimen for the tensile loading test by welding a 10K flange (SS400) on an STK400 steel pipe (inner diameter d=190.7mm, wall thickness t=5.3 mm) was created. The length of the test specimen is 1044 mm (steel pipe section + rib + flange thickness). A torque shear bolt (S10T, M20) to connect the joint between the flanges is used. When a predetermined torque was applied, the inner sleeve pintail broke off; thus, the axial force introduced in the bolt could be determined.

Figure 13 shows an overview of the tensile loading test. A 3 MN structured testing machine for the tensile loading test was used. The load in a stepwise fashion in the tensile loading test increases until a failure occurred at any point. The tensile loading test on three test specimens to ensure reproducibility was carried out.

5.2 Test results on tensile test

Figure 14 shows the relationships between the tensile load and tensile displacement in the tensile loading test. The tensile displacement to be the average of the values measured at eight points above and below the flange (= 4 points × 2) was taken. Although the tensile loading test on three test specimens (Nos. 1 ~ 3) was performed, the relationships between the tensile load and tensile displacement were almost the same for all of them. The maximum tensile load value during the test was recorded just before failure at about 1400kN.

With regard to the deformation of the test specimen, the initial stiffness could not be maintained from about 800kN, after which the deformation increased with the tensile load. Figure 15 shows the relationships between the tensile load and strain. At the centre of the steel pipe (sections 2 and 4) away from the flange as shown in Figure 15(b), the measured strain maintained the initial stiffness. However, near the flanges of the steel pipe (sections 1 and 3) as shown in Figure 15(a), a change was observed in the measured strain at about 800kN.

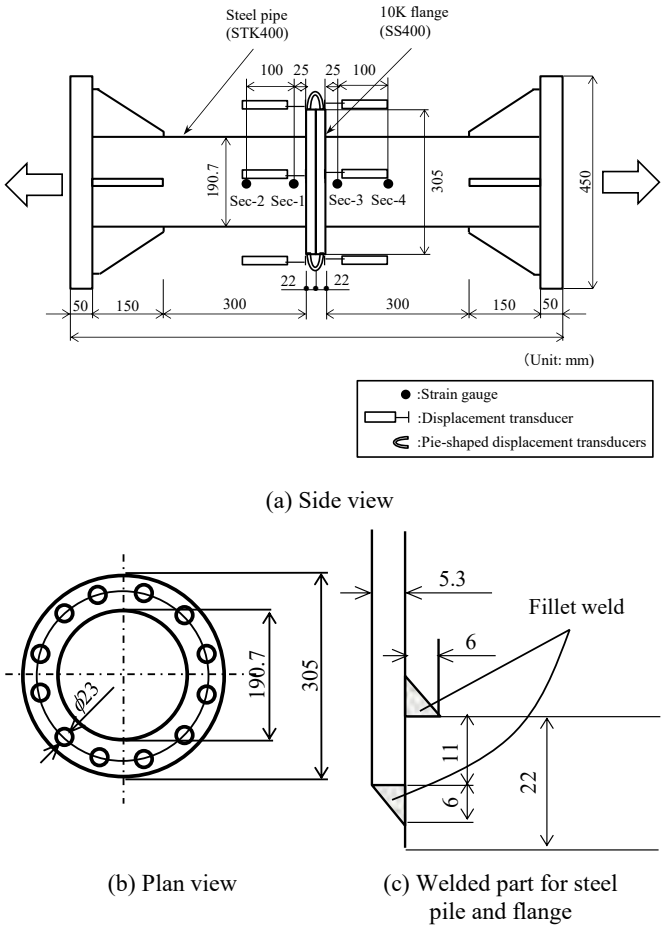

Figure 14 Overview of test specimen for tensile loading test

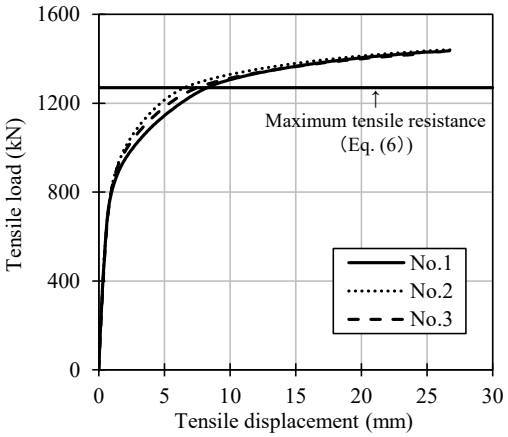

Figure 15 Relationships between tensile load and tensile displacement

Figure 16 indicates the relationships between the tensile load and displacement at flange. The flange displacement signifies the separation between the flanges, which was measured with pie-shaped displacement transducers at four points. As the tensile load increased, the displacement between the flanges indicated compressed values. Based on the above test results, the decreased

stiffness of the test specimen was due to the bending deformation of the flange. In addition, the measured strain began to increase at the centre of the steel pipe at a load of about 1200kN, which was close to the value obtained by multiplying the cross-sectional area of the steel pipe with the tensile strength obtained from the material test results.

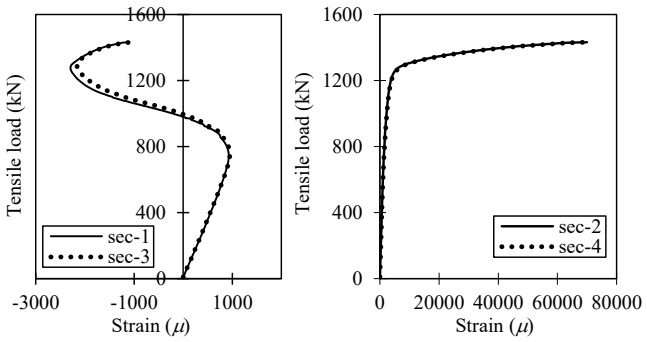

(a) Sec-1 and 3 (b) Sec-2 and 4

Figure 16 Relationships between Tensile load and strain

The failure condition of the test specimen in the tensile loading test is shown in Photo 2. After the tensile loading test, the inner periphery of the flange was separated. The flange underwent bending deformation with the area around the outer periphery as its fulcrum, and the joint bolt also underwent bending deformation. Furthermore, the diameter of the steel pipe at the centre portion was reduced. All of the test specimens appeared to fail from failure of the steel pipe at the heat-affected zone near the welded portion of the flange and steel pipe.

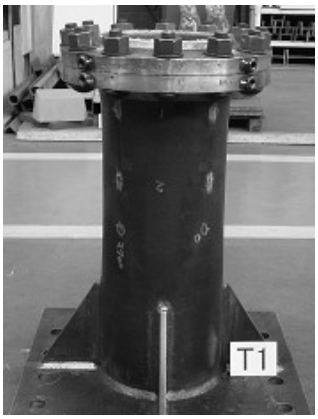

Photo 2 Failure mode of test specimen

The maximum strength obtained in the tensile loading tests and the value obtained from the calculation formula which is proposed in the "Architectural Institute of Japan: Recommendation for Design of Connection in Steel Structures (2006)" were compared. The maximum strength T_u of a flange joint of a steel pipe without ribs is given in Eq. (6).

$$T_u = \min\,(T_{u1},\ T_{u2},\ T_{u3},\ T_{u4}) \tag{6}$$

Because T_{u4} is for a localized failure mechanism when the number of bolts is small, it is evaluated T_{u1}, T_{u2}, and T_{u3} as the maximum strengths of the tensile loading tests. T_{u1}, T_{u2}, and T_{u3} can be determined by using Eqs. (7) ~ (10). All of these equations assume the three failure mechanisms shown in Figure 17 and can be derived from the force–equilibrium conditions of the axisymmetric failure mechanism.

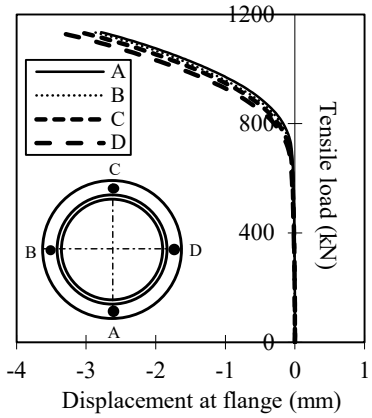

Figure 17 Relationships between tensile load and displacement at flange

$$T_{u1} = np_{bu} \tag{7}$$

$$T_{u2} = \frac{1}{\phi_f - \phi_p}\left\{(\phi_f - \phi_b)np_{bu} + (\phi_f - \phi_h)2\pi \cdot M_u\right\} \tag{8}$$

$$T_{u3} = \frac{2\phi_b - \phi_h}{\phi_b - \phi_p} 2\pi \cdot M_u \tag{9}$$

$$M_u = \frac{{t_f}^2}{4} F_{fu} \tag{10}$$

where n is the number of bolts, ϕ_f is the outer diameter of the flange, ϕ_h is the outer diameter of the flange hole, ϕ_p is the inner diameter of the steel pipe (i.e., outer diameter – wall thickness), ϕ_b is the bolt centre-to-centre diameter, t_f is the flange thickness, F_{fu} is the tensile strength of the flange, M_u is the ultimate bending strength, and p_{bu} is the maximum tensile strength of a single high-tensile bolt.

The maximum strength of the joint was calculated to be as follows;

T_{u1} = 2940kN, T_{u2} = 1270kN, and T_{u3} = 1291kN

Therefore, the maximum strength T_u of the joint used for this construction method was 1270kN. Compared with the maximum strength of 1400kN (Figure 14) obtained from the tensile loading test results, it is confirmed that the joint possessed equal or greater maximum strength.

Considering that the failure mode of the tensile loading test corresponded to mechanisms Mode 2 or Mode 3 in Figure 18, the failure mode and maximum strength generally corresponded with each other. The calculation formula given in Eq. (6) can be applied to evaluating the maximum strength of the joints used in this construction method. Here, it is said that the maximum tensile resistance of pile should not exceed the tensile resistance of joint part when the tensile resistance acts to the pile.

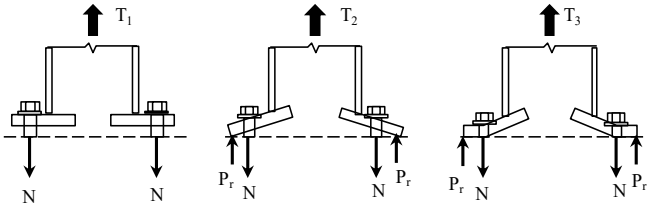

(a) Mode 1 (b) Mode 2 (c) Mode 3

Figure 18 Failure mechanism of flange

6. CONCLUSIONS

A construction method for steel pipe piles combined with ground improvement in narrow spaces was developed. In addition to evaluating the bearing capacity, the accuracy of the simplified rapid loading test used for verifying the bearing capacity onsite were confirmed.

1) The ultimate friction of the pile constructed with this method can be evaluated by considering it to be equivalent to the undrained shear strength of the ground. The bearing capacity factor related to the ultimate bearing capacity was found to be greater than 150. The above ultimate shaft friction and ultimate bearing capacity were used to propose a calculation formula for the ultimate bearing capacity of each pile type.
2) To verify the bearing capacity after construction, a simplified rapid load test as an alternative to the conventional rapid loading test was developed and verified its applicability. The results confirmed that the simplified rapid load test has sufficient accuracy for the long-term load level and is an effective quality control technique. Thus, it is said that the simplified rapid load test can apply to the real pile to confirm the bearing capacity in the long-term load level.
3) The tensile strength of the steel pipe pile joint was verified. The results showed that the joint possessed a maximum strength that was greater than or equal to the maximum strength obtained from the calculation formula. Therefore, the joint method used in this construction method is practical, and the existing calculation formula can be applied to evaluating the maximum strength of the joint.

7. REFERENCES

Architectural Institute of Japan. (2001) "Recommendation for Design of Building Foundations" (in Japanese).

Architectural Institute of Japan. (2006) " Recommendation for Design of Connection in Steel Structures " (in Japanese).

Japanese Geotechnical Society. (2001) "Standards of the Japanese Geotechnical Society (Method for Vertical Load Test of Piles)" (in Japanese).

Kitade, K., Watanabe, K., Yamamoto, T. and Kubo, T. (2012) "Verification of the improvement effect of the ground improvement structure constructed using a low-overhead clearance ground improvement method". Proceedings of the 67th Annual Conference of the Japan Society for Civil Engineers, pp799-800 (in Japanese).

Yamamoto, T., Watanabe, K., Sakahira, Y. and Moriwaki, T. (2011) "Development of steel pipe piles combined ground improvement (Part 2: Rapid loading test results)", Proceedings of the 46th Annual Meeting of the Japanese Geotechnical Society, pp1301–1302 (in Japanese).

Watanabe, K., Ishii, Y., Sudo, T., and Arakawa, M. (2011) "Development of steel pipe piles combined ground improvement (Part 1: Static loading test results)", Proceedings of the 46th Annual Meeting of the Japanese Geotechnical Society, pp1299–1300 (in Japanese).